MECHANISM STUDY OF HIGHLY ORDERED JETS IN AN IMPROVED ELECTROSPINNING PROCESS

by

Lulu GAO, Yi WANG, and Lan XU*

National Engineering Laboratory for Modern Silk, College of Textile and Clothing Engineering, Soochow University, Suzhou, China

Original scientific paper
https://doi.org/10.2298/TSCI200124122G

An improved electrospinning is suggested by placing two positively charged rings between the needle and the parallel electrode collector to fabricate highly ordered nanofibers. The theoretical analysis and experimental study were performed to investigate the mechanism of highly ordered jets in the spinning process. The influence of the distance between two rings on the product's properties was analyzed theoretically and verified experimentally. The results illustrated the addition of two rings with the optimal distance between them could further improve the ordered degree of nanofibers.

Key words: *electrospinning, nanofiber, ordered degree, theoretical model, mechanical mechanism*

Introduction

Electrospinning (ES) is a spinning method in which polymer solutions or melts are sprayed under the action of static electricity to obtain micro/nano scale fibers. The advantages of ES technology are that it is easy to prepare materials with large specific surface area, many types of polymer materials can be used, the fabricated fiber structure has high uniformity and the cost is low [1]. Therefore, it can be applied to many fields, such as tissue engineering [2], drug release [3], biomimetic materials [4], sensors [5], optoelectronic devices [6], and super-hydrophilic or super-hydrophobic surfaces [7].

Most researchers obtained oriented nanofibers from an improved spinning apparatus [8-19]. There are two ways of improving the collection device to obtain ordered fibers. One is to use a rotating object as the grounded collector [13, 14], the other is the parallel electrode method (PEM) [15-19], which fabricates aligned nanofibers by using static and separated conductive electrodes. When the two collecting electrodes are placed in parallel, the fibers are subjected to electric forces during the falling process, they are straightened and deposited between the collecting electrodes, and finally they are carried between the two electrodes. However, with the increase of spinning time PEM will seriously reduce the alignment of electrospun nanofibers. Therefore, a modified PEM by placing a positively charged ring between the needle and the parallel electrodes was applied to improve the diameter distribution and the ordered degree of nanofibers, and the highest ordered degree of nanofibers could reach 72.7% [1]. A modified bubble-ES by placing a positively charged ring between the bubble and the parallel electrode collector was also presented to fabricate highly aligned nanofibers in quanti-

* Corresponding author, e-mail: lanxu@suda.edu.cn

ties [20]. In addition, it is very significant for understanding the movement of the jet and the formation mechanism of nanofibers in the ES process, resulting in the appearance of many related researches [21-23].

In this paper, an improved PEM (IPEM) by placing two positively charged rings between the needle and the parallel electrode collector was presented to further enhance the ordered degree of nanofibers. The schematic of the IPEM apparatus was represented in fig. 1, which consists of a syringe, a needle, a parallel electrode collector, a flow meter, two copper rings with the diameter of 24 cm and two variable DC high voltage generators. The needle tip is connected to the positive pole of the first generator, and the parallel electrode collector is connected to the negative pole of the same generator. The voltage provided by the generator is called the applied voltage. The positive terminal of the second generator is respectively connected to the two copper rings through two copper wires, and the voltage provided is called the ring voltage. The theoretical analyses and experimental researches were used to study the mechanical mechanism of highly ordered jets in the IPEM process. The influence of the distance between two rings on the electrospun nanofibers was analyzed theoretically, and was verified experimentally by measuring the diameter distribution and the ordered degree of nanofibers. The theoretical analyses were in good agreement with the experimental data. The results showed that the addition of two rings with the optimal distance between them could further improve the ordered degree of nanofibers compared with the addition of one ring.

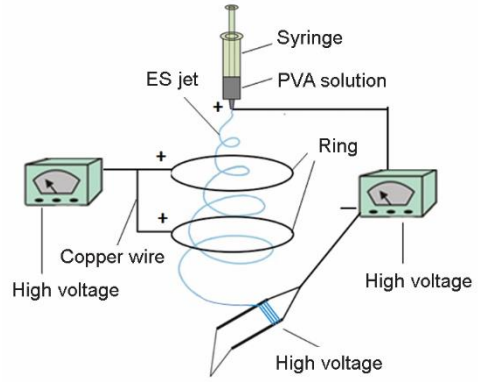

Figure 1. Schematic of the IPEM apparatus

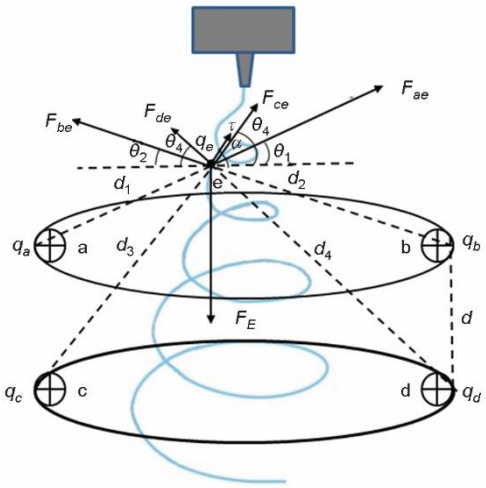

Figure 2. Application of two positively charged rings to the electrospinning

Theoretical analysis

When two positively charged rings were placed between the needle and the parallel electrode collector, fig. 2, Coulomb forces were generated due to the current in the polymer jet [1]:

$$F_{ae} = \frac{kq_a q_e}{d_1^2}, \quad F_{be} = \frac{kq_b q_e}{d_2^2}, \quad F_{ce} = \frac{kq_c q_e}{d_3^2}, \quad F_{de} = \frac{kq_d q_e}{d_4^2} \tag{1}$$

where k is the Coulomb's constant ($k = 8.987552 \cdot 10^9$ Nm^2/C^2), q_e – the signed magnitude of the point e charge, q_a, q_b, q_c, and q_d – the electric charges transferred through the ring over a time t, d_1 – the distance between the charges q_a and q_e, d_2 – the distance between the charges q_b and q_e, d_3 – the distance between the charges q_c and q_e, and d_4 – the distance between the charges q_d and q_e. The vector forms in these equations represented respectively the force F_{ae}

applied on q_e by q_a the force F_{be} applied on q_e by q_b, the force F_{ce} applied on q_e by q_c, and the force F_{de} applied on q_e by q_d.

Analysis of the vertical components of forces

Figure 3 shows the vertical components of forces at the point *e* in the IPEM process.

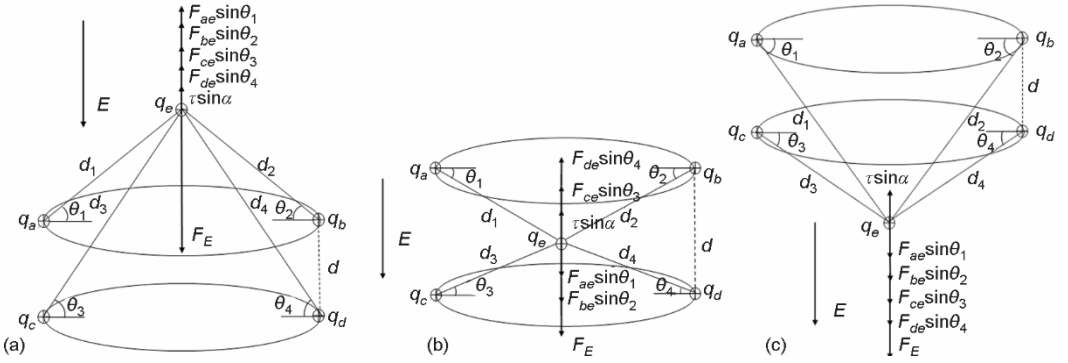

Figure 3. Analysis of the vertical components of forces at the point *e*; (a) from the needle to the first ring, (b) from the first ring to the second ring, and (c) from the second ring to the collector

In fig. 3(a), the vertical resultant force F_1 could be calculated in the following form:

$$F_1 = F_E - F_{ae}\sin\theta_1 - F_{be}\sin\theta_2 - F_{ce}\sin\theta_3 - F_{de}\sin\theta_4 - \tau\sin\alpha =$$

$$= F_E - \frac{kq_aq_e}{d_1^2}\sin\theta_1 - \frac{kq_bq_e}{d_2^2}\sin\theta_2 - \frac{kq_cq_e}{d_3^2}\sin\theta_3 - \frac{kq_dq_e}{d_4^2}\sin\theta_4 - \tau\sin\alpha \tag{2}$$

where F_E is the electric field force and τ – the viscous force.

$$F_E = q_eE \tag{3}$$

$$\tau = av + bv^2 \tag{4}$$

where E is the electric field intensity, a and b – the constants to be further determined experimentally or theoretically, and v – the velocity of the jet.

$$\mathrm{E} = \frac{U}{d} \tag{5}$$

$$q_a = q_b = q_c = q_d = \frac{U_0}{R}t \tag{6}$$

where U is the voltage (or potential difference) between the needle and the collector, d – the distance from the needle to the collector, U_0 – the applied ring voltage, and R – the electrical resistance of the ring.

Putting eqs. (3)-(6) into eq. (2), F_1 could be written:

$$F_1 = q_eE - \frac{kq_aq_e}{d_1^2}\sin\theta_1 - \frac{kq_bq_e}{d_2^2}\sin\theta_2 - \frac{kq_cq_e}{d_3^2}\sin\theta_3 - \frac{kq_dq_e}{d_4^2}\sin\theta_4 - (av + bv^2)\sin\alpha =$$

$$= q_e\left[\frac{U}{d} - \frac{ktU_0}{R}\left(\frac{\sin\theta_1}{d_1^2} + \frac{\sin\theta_2}{d_2^2} + \frac{\sin\theta_3}{d_3^2} + \frac{\sin\theta_4}{d_4^2}\right)\right] - (av + bv^2)\sin\alpha \tag{7}$$

Suppose the vertical component of viscous force contributes no work for the downward movement of the jet. Then F_1 could be written:

$$F_1 = q_e\left[\frac{U}{d} - \frac{ktU_0}{R}\left(\frac{sin\theta_1}{d_1^2} + \frac{sin\theta_2}{d_2^2} + \frac{sin\theta_3}{d_3^2} + \frac{sin\theta_4}{d_4^2}\right)\right] \tag{8}$$

According to eq. (8), the vertical resultant force produced by the two rings:

$$F_r = q_e\frac{ktU_0}{R}\left(\frac{\sin\theta_1}{d_1^2} + \frac{\sin\theta_2}{d_2^2} + \frac{\sin\theta_3}{d_3^2} + \frac{\sin\theta_4}{d_4^2}\right)$$

would hinder the downward movement of the charged jet. When

$$\frac{U}{d} < \frac{ktU_0}{R}\left(\frac{\sin\theta_1}{d_1^2} + \frac{\sin\theta_2}{d_2^2} + \frac{\sin\theta_3}{d_3^2} + \frac{\sin\theta_4}{d_4^2}\right), \text{ that was } F_1 < 0,$$

F_1 would hinder the downward movement of the charged jet. When

$$\frac{U}{d} > \frac{ktU_0}{R}\left(\frac{\sin\theta_1}{d_1^2} + \frac{\sin\theta_2}{d_2^2} + \frac{\sin\theta_3}{d_3^2} + \frac{\sin\theta_4}{d_4^2}\right), \text{ that was } F_1 > 0,$$

the downward movement of the charged jet would be accelerated byF_1, and the stability condition was improved. When:

$$\frac{U}{d} = \frac{ktU_0}{R}\left(\frac{\sin\theta_1}{d_1^2} + \frac{\sin\theta_2}{d_2^2} + \frac{\sin\theta_3}{d_3^2} + \frac{\sin\theta_4}{d_4^2}\right)$$

F_1 contributes no work for the moving jet. Therefore, well-aligned nanofibers would be obtained by adjusting the applied ring voltages and the distance between the two rings in the IPEM process.

In figs. 3(b) and 3(c), proceeding the same way as illustrated in fig. 3(a), the vertical resultant forces F_2 and F_3 could be also calculated, respectively:

$$F_2 = q_e\left[\frac{U}{d} + \frac{ktU_0}{R}\left(\frac{\sin\theta_1}{d_1^2} + \frac{\sin\theta_2}{d_2^2} - \frac{\sin\theta_3}{d_3^2} - \frac{\sin\theta_4}{d_4^2}\right)\right] \tag{9}$$

$$F_3 = q_e\left[\frac{U}{d} + \frac{ktU_0}{R}\left(\frac{\sin\theta_1}{d_1^2} + \frac{\sin\theta_2}{d_2^2} + \frac{\sin\theta_3}{d_3^2} + \frac{\sin\theta_4}{d_4^2}\right)\right] \tag{10}$$

In view of eq. (9) and fig. 3(b), it could be found the electric field forces provided respectively by the two rings, that are:

$$F_{r1} = q_e\frac{ktU_0}{R}\left(\frac{\sin\theta_1}{d_1^2} + \frac{\sin\theta_2}{d_2^2}\right), \quad \text{and} \quad F_{r2} = q_e\frac{ktU_0}{R}\left(\frac{\sin\theta_3}{d_3^2} + \frac{\sin\theta_4}{d_4^2}\right)$$

substantially cancel each other out. Therefore, F_2 is basically equal to the electric field force F_E. It could be seen from eq. (10) and fig. 3(c) that the vertical resultant force F_r produced by the two rings would increase the kinetic energy of the moving jet, and the downward movement of the jet would be accelerated by F_3.

Analysis of the horizontal components of forces

Figure 4 showed the horizontal components of forces at the point *e* in the IPEM process. As indicated in figs. 4(a)-(c), all of horizontal resultant forces F_4 could be written as follows:

$$F_4 = \tau\cos\alpha + F_{ae}\cos\theta_1 + F_{ce}\cos\theta_3 - F_{be}\cos\theta_2 - F_{de}\cos\theta_4 \tag{11}$$

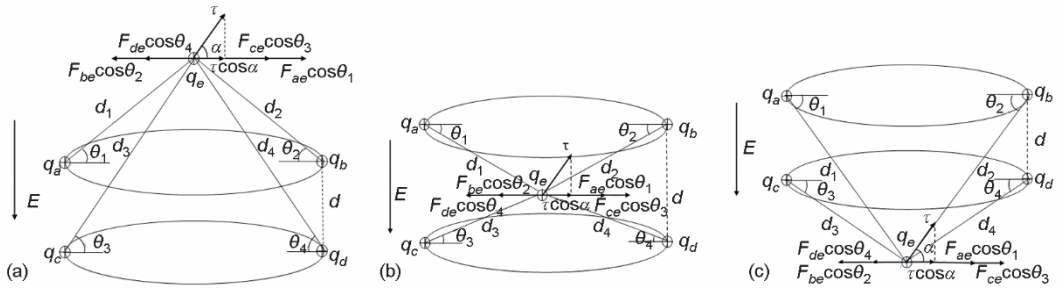

Figure 4. Analysis of the horizontal components of forces at the point *e*; (a) from the needle to the first ring, (b) from the first ring to the second ring, and (c) from the second ring to the collector

Substituting eqs. (1) and (4) into eq. (11), the resulting horizontal resultant force F_4 could be written in the following form:

$$F_4 = (av + bv^2)\cos\alpha + kq_e\left(\frac{q_a\cos\theta_1}{d_1^2} + \frac{q_c\cos\theta_3}{d_3^2} + \frac{q_b\cos\theta_2}{d_2^2} + \frac{q_d\cos\theta_4}{d_4^2}\right) \tag{12}$$

The horizontal resultant force F_4 produced a centripetal force, which would shrink the radius of whipping circle, leading to the less energy waste in the instability process and the increase of the kinetic energy of the moving jet [24]. Therefore, the stability condition of the jet and the ordered degree of nanofibers would be apparently improved.

Experimental verification

The aforementioned theoretical results would be verified by the experimental research. Polyacrylonitrile (PAN) was dissolved in the N, N-dimethylformamide (DMF) with a concentration of 10 wt.% for preparing the spinning solution. All the experiments were performed with the applied voltage of 18 kV, the flow rate of 0.1 mL/h, the collective distance 28 cm, the applied ring voltage of 5 kV and the distance from the second ring to the parallel electrode collector of 10 cm at room temperature of 25 ºC and relative humidity of 45%. In order to study the effect of the distance between the two rings on the ordered degree of nanofibers, the distance between the first ring and the second ring varied from 2 to 8 cm.

The morphologies of nanofibers produced by IPEM with the different distances between the two rings were investigated respectively by SEM. The SEM micrographs and their corresponding diameter distributions of nanofibers obtained were shown in fig. 5. It could be seen that IPEM can easily produce highly aligned nanofibers with uniform diameter distribution. The average diameters of the nanofibers prepared using different distances between the two rings, such as 2 cm, 4 cm, 6 cm, and 8 cm, were 617 ± 19.05 nm, 475 ± 17.07 nm, 613 ± 15.07 nm, and 642 ± 17.44 nm, respectively. The ordered degrees of the nanofibers obtained using different distances between the two rings were respectively 50%, 50%, 82%, and 54%. The results indicated that when the distance between the two rings was 6 cm the prepared nanofibers had the most uniform diameter distribution and the highest ordered degree.

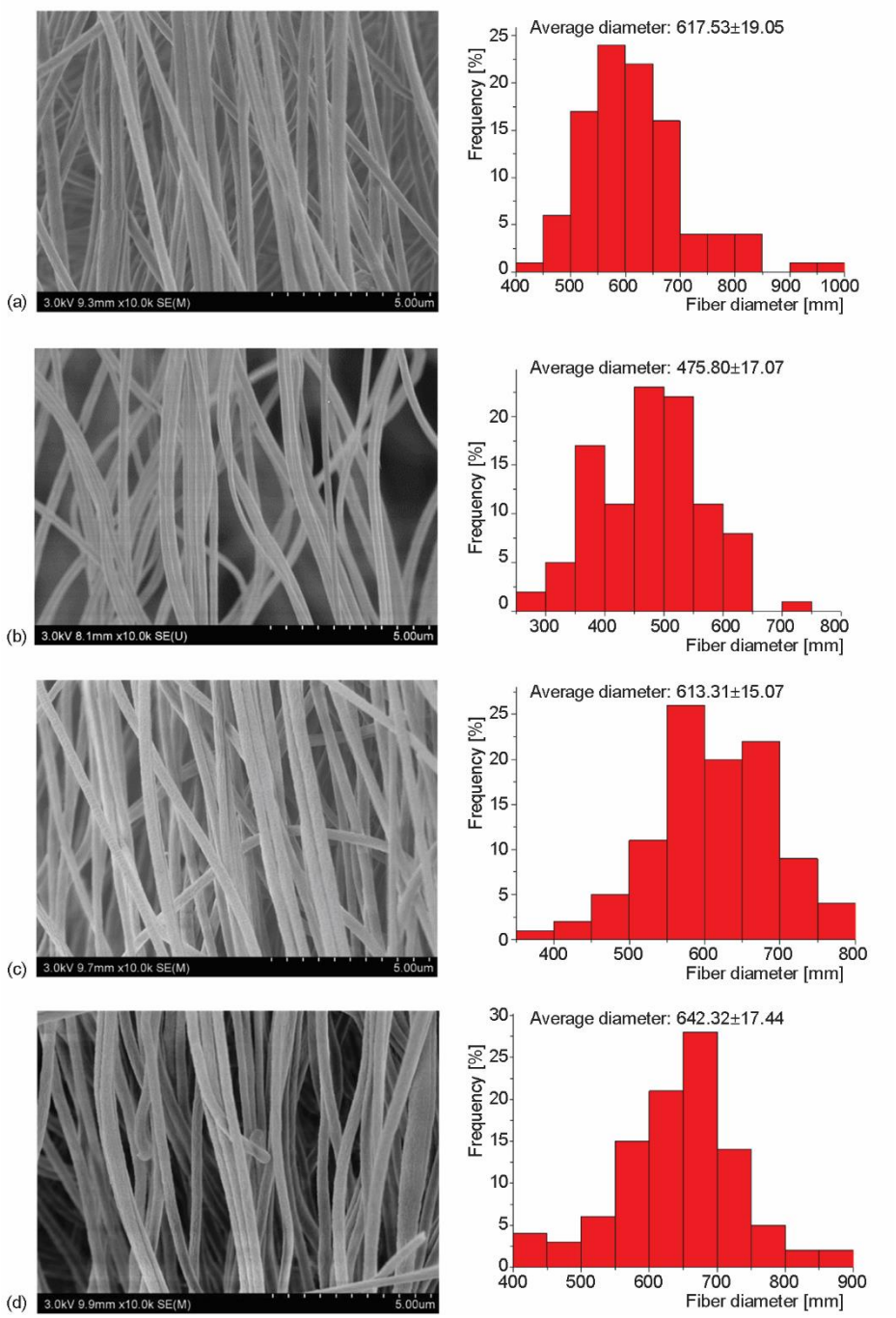

Figure 5. The SEM images and diameter distributions of the obtained nanofibers with different distance between the two rings; (a) 2cm, (b) 4cm, (c) 6cm, and (d) 8cm

In view of figs. 2 and 3, when d, d_3, and d_4 is kept constant, as the distance between the two rings varies, d_1 and d_2 will change accordingly. According to fig. 3(a) and eq. (8), as the distance between the two rings increased, d_1 and d_2 increased, then F_r decreased, resulting in the increase of F_1, which would accelerate the downward movement of the jet and enhance the ordered degree of nanofibers produced. However, when the distance between the two rings was too large, according to fig. 3(c) and eq. (10), F_3 would decrease a lot, it would cause the decrease of the ordered degree of nanofibers. Therefore, there was an optimal distance between the two rings, which was 6 cm according to the experimental results. The theoretical analysis results were in good agreement with the experimental data, indicating that IPEM can be used to optimize and control the ordered degrees of electrospun nanofibers.

Conclusion

In this paper, an IPEM was successfully developed, which could produce highly aligned electrospun nanofibers by placing two positively charged rings between a needle and a parallel electrode collector. The theoretical analyses were performed to research the mechanical mechanism of highly ordered jets in the IPEM process. And the effect of the distance between the two rings on the product quality, such as diameter and ordered degree was analyzed theoretically, and was verified experimentally by measuring the diameter distribution and the ordered degree of nanofibers. The experimental data were in keeping with the theoretical analysis results, and illustrated the IPEM could enhance the ordered degrees of electrospun nanofibers, and the addition of two rings with the optimal distance between them of 6 cm could further improve the ordered degree of nanofibers compared with the addition of one ring, which could achieve a ordered degree of 82%. The IPEM method can be extended to other modifications of electrospinning [25-32].

Acknowledgment

The work is supported financially by National Natural Science Foundation of China (Grant No. 11672198), PAPD (A Project Funded by the Priority Academic Program Development of Jiangsu Higher Education Institutions), and Six Talent Peaks Project of Jiangsu Province (Grant No. GDZB-050).

References

[1] Zhao, J. H., *et al.*, Preparation and Formation Mechanism of Highly Aligned Electrospun Nanofibers Using a Modified Parallel Electrode Method, *Materials & Design, 90* (2016), Jan., pp. 1-6
[2] Mehrasa, M., *et al.*, Electrospun Aligned PLGA and PLGA/Gelatin Nanofibers Embedded with Silica Nanoparticles for Tissue Engineering, *International Journal of Biological Macromolecules, 79* (2015), Aug., pp. 687-695
[3] Eslamian M., *et al.*, Electrospinning of Highly Aligned Fibers for Drug Delivery Applications, *Journal of Materials Chemistry B, 7* (2019), 2, pp. 224-232
[4] Bhutto, M. A., *et al.*, Development of Poly (L-Lactide-Co-Caprolactone) Multichannel Nerve Conduit with Aligned Electrospun Nanofibers for Schwann Cell Proliferation, *International Journal of Polymeric Materials and Polymeric Biomaterials, 65* (2016), 7, pp. 323-329
[5] Fu, W., *et al.*, Electronic Textiles Based on Aligned Electrospun Belt-Like Cellulose Acetate Nanofibers and Graphene Sheets: Portable, Scalable and Eco-Friendly Strain Sensor, *Nanotechnology, 30* (2019), 4, ID 045602
[6] Buyukanir, E. A., *et al.*, Optically Responsive Nematic Liquid Crystal/Polymer Core-Shell Fibers: Formation and Characterization, *Polymer, 51* (2010), 21, pp. 4823-4830
[7] Ding, B., *et al.*, Conversion of an Electrospunnanofibrous Cellulose Acetate Mat from a Super-Hydrophilic to Super-Hydrophobic Surface, *Nanotechnology, 17* (2006), 17, pp. 4332-4339

[8] Yang, D., *et al.*, Aligned Electrospun Nanofibers Induced by Magnetic Field, *Journal of Applied Polymer Science, 110* (2008), 6, pp. 3368-3372
[9] Zhang, Q. C., *et al.*, Large-Scale Aligned Fiber Mats Prepared by Salt-Induced Pulse Electrospinning, *Journal of Polymer Science, Part B: Polymer Physics, 50* (2012), 14, pp. 1004-1012
[10] Sarkar, S., *et al.*, Electrospinning of Aligned Polymer Nanofibers, *Macromolecular Rapid Communications, 28* (2007), 9, pp. 1034-1039
[11] Heidari, I., *et al.*, A Novel Approach for Preparation of Aligned Electrospunpolyacrylonitrile Nanofibers, *Chemical Physics Letters, 590* (2013), Dec., pp. 231-234
[12] Erickson, A. E., *et al.*, High-Throughput and High-Yield Fabrication of Uniaxially-Aligned Chitosan-Based Nanofibers by Centrifugal Electrospinning, *Carbohydrate Polymers, 134* (2015), Dec., pp. 467-474
[13] Katta, P., *et al.*, Continuous Electrospinning of Aligned Polymer Nanofibers Onto a Wire Drum Collector, *Nano Letters, 4* (2004), 11, pp. 2215-2218
[14] Theron, A., *et al.*, Electrostatic Field-Assisted Alignment of Electrospun Nanofibers, *Nanotechnology, 12* (2001), 3, pp. 384-390
[15] Ishii, Y., *et al.*, A New Electrospinning Method to Control the Number and a Diameter of Uniaxially Aligned Polymer Fibers, *Materials Letters, 62* (2008), 19, pp. 3370-3372
[16] Song, Y. H., *et al.*, Fabrication and Characterization of Magnetic Nanocomposites by Electric Fields Assisted Electrospinning, *Thermal Science, 23* (2019), 4, pp. 2365-2372
[17] Rein, D. M., *et al.*, Electrospinning of Ultrahigh-Molecular-Weight Polyethylene Nanofibers, *Journal of Polymer Science, Part B: Polymer Physics, 45* (2007), 7, pp. 766-773
[18] Song, Y. H., *et al.*, Preparation and Characterization of Highly Aligned Carbon Nanotubes/Polyacrylonitrile Composite Nanofibers, *Polymers*, 9 (2017), 1, pp. 1-13
[19] Yang, D., *et al.*, Fabrication of Aligned Fibrous Arrays by Magnetic Electrospinning, *Advanced Materials, 19* (2007), 21, pp. 3702-3706
[20] Shao, Z. B., *et al.*, Formation Mechanism of Highly Aligned Nanofibers by a Modified Bubble-Electrospinning, *Thermal Science, 22* (2018), 1A, pp. 5-10
[21] Xu, L. ,A Particle Suspension Model for Nanosuspensions Electrospinning, *Thermal Science, 22* (2018), 4, pp. 1707-1714
[22] He, J.-H., *et al.*, Review on Fiber Morphology Obtained by Bubble Electrospinning and Blown Bubble Spinning, *Thermal Science, 16* (2012), 5, pp. 1263-1279
[23] Xu, L., *et al.*, Numerical Simulation for the Single-Bubble Electrospinning Process, *Thermal Science, 19* (2015), 4, pp. 1255-1259
[24] Liu, H. Y., *et al.*, Effect of Magnetic Intensity on Diameter of Charged Jets in Electrospinning, *Thermal Science, 18* (2014), 5, pp. 1451-1454
[25] Li, X. X., *et al.*, The Effect of Sonic Vibration on Electrospun Fiber Mats, *Journal of Low Frequency Noise Vibration and Active Control, 38* (2019), 3-4, pp. 1246-1251
[26] Zhao, J. H., *et al.* Needle's Vibration in Needle-Disk Electrospinning Process: Theoretical Model and Experimental Verification, *Journal of Low Frequency Noise Vibration and Active Control, 38* (2019), 3-4, pp. 1338-1344
[27] Yin, J., *et al.*, Numerical Approach to High-Throughput of Nanofibers by a Modified Bubble-Electrospinning, *Thermal Science, 24* (2020), 4, pp. 2367-2375
[28] Ahmed, A., Xu, L., Numerical Analysis of the Electrospinning Process for Fabrication of Composite Fibers, *Thermal Science, 24* (2020), 4, pp. 2377-2383
[29] Li, X. X., *et al.*, Nanofibers Membrane for Detecting Heavy Metal Ions, *Thermal Science, 24* (2020), 4, pp. 2463-2468
[30] Yao, X., He, J.-H., On Fabrication of Nanoscale Non-Smooth Fibers with High Geometric Potential and Nanoparticle's Non-Linear Vibration, *Thermal Science, 24* (2020), 4, pp. 2491-2497
[31] He, J.-H., On the Height of Taylor Cone in Electrospinning, *Results in Physics, 17* (2020), June, ID 103096
[32] Wu, Y. K., Liu, Y., Fractal-Like Multiple Jets in Electrospinning Process, *Thermal Science, 24* (2020), 4, pp. 2499-2505

Paper submitted: January 24, 2020
Paper revised: July 1, 2020
Paper accepted: July 1, 2020